Transition probabilities and interacting boson-fermion model description of positive parity states in ^{117}Sb

Yu. N. Lobach
Institute for Nuclear Research, pr. Nauki 47, 252028 Kiev, Ukraine

D. Bucurescu
Horia Hulubei National Institute of Physics and Nuclear Engineering, Bucharest, Romania
(Received 11 May 1998)

The Doppler shift attenuation method was used to determine lifetimes in the picosecond region for excited states of ^{117}Sb populated with the $(\alpha,2n\gamma)$ reaction at $E_\alpha=27.2$ MeV. Interacting boson-fermion model calculations explain reasonably well the main features of the positive parity levels known up to about 2.5 MeV excitation. The mixing of the lowest one-quasiparticle $9/2^+$ state with the intruder $(2p\text{-}1h)$ $9/2^+$ state, as well as the quadrupole deformation of the intruder band are also discussed. [S0556-2813(98)03809-6]

PACS number(s): 21.10.Tg, 21.60.Fw, 23.20.Lv, 27.60.+j

I. INTRODUCTION

The nuclei in the single closed shell region have been traditionally regarded as characterized by two main excitation modes, the single particle and the collective vibrations around the equilibrium shape. The odd-A antimony nuclei possess a variety of spherical states obtained by coupling an odd valence proton occupying the $\pi g_{7/2}$, $\pi d_{5/2}$, and $\pi h_{11/2}$ orbitals to states of the neighboring Sn core nuclei. Moreover, rotational bands based on a $9/2^+$ state have been commonly observed in odd-A Sb isotopes [1] from the excitation of a $g_{9/2}$ proton across the $Z=50$ closed shell. These peculiarities of the odd-A antimony nuclei have generated a great deal of interest in the study of their structure during the last few years [2–10]. The ^{117}Sb nucleus is a good example of such detailed spectroscopic investigations. Thus, the structure of this nucleus was studied with the $(p,n\gamma)$ [11,12], $(p,2n\gamma)$ [13], $(\alpha,2n\gamma)$ [11,14,15], (^{6}Li,$3n\gamma$) [1], (^{11}B,$4n\gamma$) [9,10], and (^{3}He,d) reactions [16]. As a result of these works, valuable information was obtained about the energy levels of ^{117}Sb and their spin, parity, and γ-decay modes [17,18]. Nevertheless, not very much information concerning the electromagnetic properties is available: only the lifetimes of long-lived isomers in the nanosecond region [11,14,19] and several lifetimes of low-spin states, measured with the $(p,n\gamma)$ reaction [20]. The study of the electromagnetic decay properties of nuclei leads to a more thorough understanding of different aspects of their structure and is helpful for further development of nuclear structure models. Therefore the aim of the present work is to extend the data on lifetimes of excited states of ^{117}Sb at middle spins in the picosecond region, by using the Doppler shift attenuation method (DSAM) in connection with the $(\alpha,2n\gamma)$ reaction.

II. EXPERIMENTAL PROCEDURE AND RESULTS

The states in ^{117}Sb were populated with the ^{115}In$(\alpha,2n\gamma)^{117}$Sb reaction at a beam energy of 27.2 MeV. The beam was provided by the U-120 cyclotron of the Institute for Nuclear Research, Kiev. The procedure was the same as that described in our recent work for ^{115}Sb [21], therefore we give here only a brief description of it.

The DSA experiment was carried out by measuring γ-ray spectra at angles of 30°, 60°, 90°, 120°, and 150° with respect to the beam direction with a high-purity germanium detector of 50% relative efficiency and 2.2 keV full width at half maximum (FWHM) energy resolution at $E_\gamma=1.33$ MeV. The self-supported enriched ^{115}In target had a thickness of 4.3 mg/cm^2. Figure 1 shows the spectrum measured at 90°; spectra with similar statistics were obtained at the other angles.

The spectra measured at different angles were used to extract mean lifetimes by applying the Doppler shift attenuation method. The level lifetimes were derived from a least squares fit of the experimental line shapes of transition γ rays from that level with calculated ones. Such calculations were performed using an updated version of the computer code described in Ref. [22]. The velocity distribution of the emitting nuclei was calculated from the simulation of 30 000 recoil histories by a Monte Carlo code which takes into account reactions at different depths of the target, the kinemat-

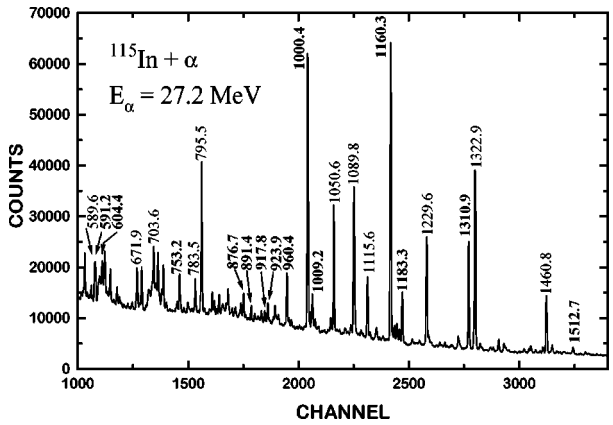

FIG. 1. Singles γ-ray spectrum of the ^{115}In$(\alpha,2n\gamma)^{117}$Sb reaction at 27.2 MeV, measured at 90°. Peaks labeled with bold letters correspond to the transitions used for lifetime determinations in the present work.

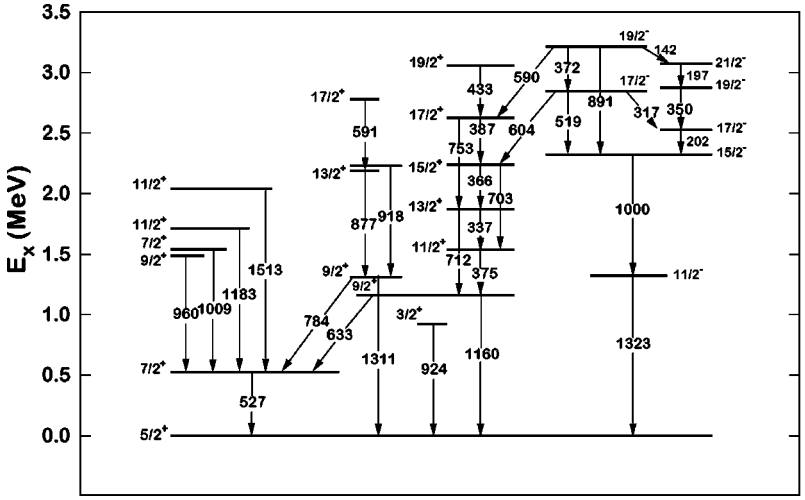

FIG. 2. Partial level scheme of ^{117}Sb, showing the decay scheme of the levels of interest in the present DSAM lifetime analysis.

ics of the reaction, as well as the slowing down and the deflection of the recoils. For the slowing-down process the Lindhard's cross sections [23] were used, with correction factors $f_e = 1.3$ and $f_n = 0.9$ for the electronic and the nuclear stopping power, respectively. These values are suggested from the analysis of the slowing-down process of Cd ions in a Cd target [24].

The cascade feeding from higher-lying levels with known lifetimes and side feeding into each level were taken into account in these calculations. The feeding pattern of each level under study was accounted for according to the level scheme of ^{117}Sb from Ref. [15]. The partial level scheme relevant for the present DSAM analyses is shown in Fig. 2. For the side-feeding times (τ_{sf}) of the investigated levels we have chosen values depending on the energy of the state and the position of the calculated entry region. The center of the entry region lies at relatively low energy, not exceeding 0.5–1.0 MeV above the states of interest, which leads to small values of τ_{sf}. In addition, we assumed an increase of τ_{sf} with a decreasing excitation energy of 0.03 ps/MeV, so, finally, the side-feeding times used (which were kept constant for each level) were in the range 0–0.06 ps, similarly to the case of ^{115}Sb [21].

As an illustration of the DSAM analysis the line shape of three γ-ray transitions are shown in Fig. 3. The lifetime values obtained from the present measurements as well as from other previous works are given in Table I. The lifetimes finally adopted in the present experiment are weighted averages of the values obtained from the measurements at different angles. The errors of the adopted lifetimes include the statistical errors, the uncertainties of the feeding time and intensities, and a 20% uncertainty due to the nuclear and electronic stopping powers.

On the basis of the measured lifetimes, the reduced electromagnetic transition probabilities $B(\sigma L)$ were calculated and are presented in Table II. The relative intensities of the γ-ray transitions and their multipole mixing ratios δ for the mixed $M1/E2$ transitions were taken from Refs. [10, 15, 18]. Unfortunately, for most of the mixed transitions the mixing ratios are unknown. In these cases the reduced transition probabilities were calculated as for pure $M1$ or $E2$ transition, respectively.

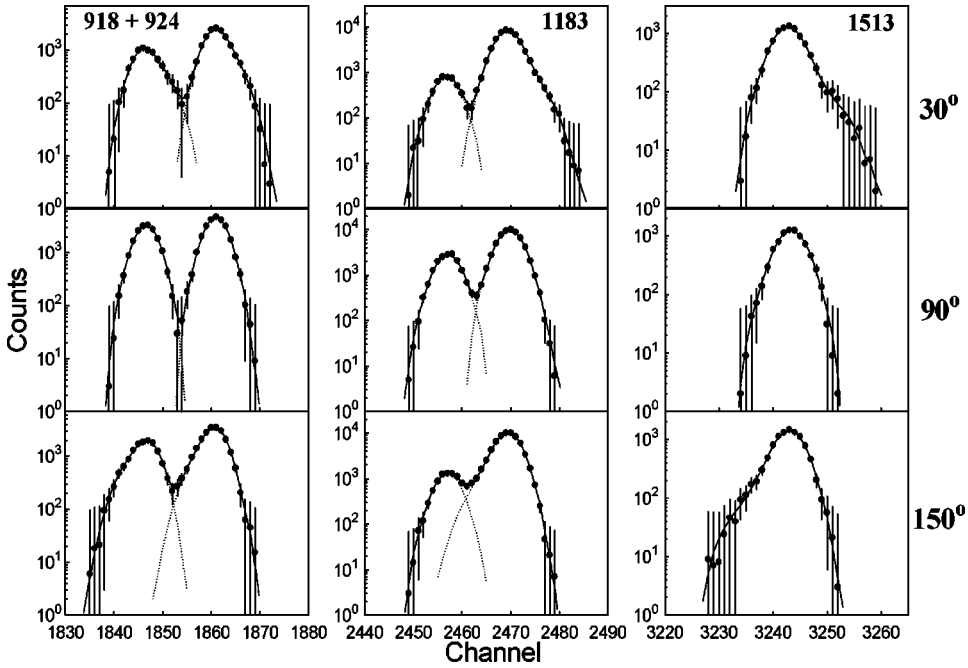

FIG. 3. Examples of Doppler shift attenuation analyses of γ-ray line shapes. Left: the 917.8 and 923.9 keV transitions; middle: the 1183.3 keV transition (close to it, a γ ray of 1178.2 keV which has no Doppler broadening); right: the 1512.3 keV transition. The dotted lines show the decomposition of the fit when there are two components (γ lines). The experimental line shapes result from the measured single spectra such as, e.g., that from Fig. 1, after subtracting a continuous background fitted to the neighboring regions which do not contain peaks.

TABLE I. Experimental lifetimes of excited states in ^{117}Sb. For the states measured in this work, the energy of the decay γ ray (E_γ) analyzed by DSAM is indicated.

E_{lev} (keV)	J^π	E_γ (keV)	τ (ps) Present	τ (ps) Ref. [20]	τ (ps) Others
923.9	$3/2^+$	923.9	$0.75^{+0.25}_{-0.20}$	$0.17^{+0.10}_{-0.05}$	
1089.4	$7/2^+$			$0.22^{+0.21}_{-0.08}$	
1160.3	$9/2^+$	1160.3	$\geqslant 3.0$		
1310.9	$9/2^+$	1310.9	2.85 ± 0.80	$\geqslant 0.08$	
1322.9	$11/2^-$				$(5.48 \pm 0.29) \times 10^3$ [a]
1378.9	(7/2)			$0.22^{+0.21}_{-0.08}$	
1471.7	(7/2)			$\geqslant 0.53$	
1487.8	$9/2^+$	960.4	1.2 ± 0.4		
1536.6	$7/2^+$	1009.2	$0.6^{+0.4}_{-0.2}$	$\geqslant 0.35$	
1623.3	(3/2)			$\geqslant 0.19$	
1710.7	$11/2^+$	1183.3	$1.95^{+0.60}_{-0.50}$		
1716.3	$(1/2,3/2)^+$			$0.046^{+0.010}_{-0.008}$	
1751.8				$0.34^{+0.45}_{-0.14}$	
2040.1	11/2+	1512.7	$2.0^{+2.0}_{-0.5}$		
2085.2				$0.095^{+0.043}_{-0.026}$	
2187.6	$13/2^+$	876.7	$1.05^{+0.60}_{-0.30}$		
2228.7		917.8	$0.7^{+0.4}_{-0.3}$		
2300.0	$(1/2,3/2)^+$			$0.020^{+0.015}_{-0.011}$	
2323.3	$15/2^-$	1000.4	$\geqslant 3.0$		
2625.1	$17/2^+$	753.2	$1.4^{+0.6}_{-0.5}$		
2778.8	$17/2^+$	591.2	$\geqslant 2.0$		
2780.4	$19/2^-$				$(7.2 \pm 2.2) \times 10^2$ [a]
2841.7	$17/2^-$	604.4	$1.6^{+0.6}_{-0.4}$		
2874.9	$19/2^-$				$\leqslant 290$[a]
3073.0	$21/2^-$				$\leqslant 140$[a]
3131.0	$25/2^+$				$(5.12 \pm 0.25) \times 10^8$ [b]
3214.7	$19/2^-$	891.4	$\geqslant 2.0$		
3230.6	$23/2^-$				$(4.18 \pm 0.07) \times 10^3$ [c]

[a]Reference [19].
[b]Reference [11].
[c]Reference [14].

III. THEORETICAL CALCULATIONS AND DISCUSSION

The low-lying level structure of ^{117}Sb is defined mainly by the odd valence proton occupying orbitals beyond the $Z = 50$ closed shell and its interaction with collective and quasiparticle excitations of the core. The most comprehensive previous calculations for the level structure of ^{117}Sb were performed in Ref. [25] within the frame of the unified model. These calculations took into account the coupling of the $3s_{1/2}$, $2d_{3/3}$, $2d_{5/2}$, $1g_{7/2}$, and $1h_{11/2}$ single-particle proton states to one or two quadrupole phonons or to one octupole phonon in the core. The predicted spectrum of excited states has a rather complex structure caused by the splitting of the different vibrational multiplets. On the whole, the calculated spectrum gave a satisfactory description of the level energies. At the same time, the calculated transition probabilities were not presented in Ref. [25] and consequently we cannot make a direct comparison between the measured and the calculated values.

In order to understand the electromagnetic decay properties of ^{117}Sb we use calculations in the framework of the interacting boson-fermion model (IBFM) in its variant IBFM-1 [26]. A first analysis of the positive parity states in ^{115,117}Sb with this model was performed in Ref. [20], and a more detailed one for ^{115}Sb in a more recent publication [21].

The present approach is similar to the previous ones [20,21]. In this model, to describe the positive parity states, we couple to the ^{116}Sn core (whose IBA-1 parametrization is given in Ref. [20]) a (proton) fermion which is allowed to occupy the $2d_{5/2}$, $1g_{7/2}$, $3s_{1/2}$, and $2d_{3/2}$ orbitals. The quasiparticle energies and shell occupancies are those provided by a BCS calculation, starting from the single particle energies of Reehal and Sorensen [27] (with the $1h_{11/2}$ orbital also included). As in Refs. [20,21], we keep in the boson-fermion interaction part of the Hamiltonian only the quadrupole-quadrupole interaction. Energy levels and transition probabilities were calculated with the codes ODDA and PBEM [28], respectively. Spectroscopic factors for the (^{3}He,d) reaction were also calculated with the code SPEC [29]. For the electromagnetic transition probability calculations, some effective charges and gyromagnetic ratios are needed. Thus, we have used a boson effective charge of 0.1 e b, which was

TABLE II. Experimental electromagnetic transition probabilities in ^{117}Sb.

E_{lev} (keV)	J_i^π	E_γ (keV)	J_f^π	σL	δ	$B(E2)$ (W.u.)	$B(M1)\times10^3$ (W.u.)	$B(E1)$ (W.u.)
923.9	$3/2^+$	923.9	$5/2^+$	$(M1+E2)$		50.0 ± 14.6[a]	60.6 ± 20.2[b]	
1089.4	$7/2^+$	1089.4	$5/2^+$	$(M1+E2)$		74.0 ± 37.6[a]	117 ± 60[b]	
1160.3	$9/2^+$	632.9	$7/2^+$	$(M1+E2)$		$\leqslant2.3$[a]	$\leqslant1.3$[b]	
		1160.3	$5/2^+$	$E2$		$\leqslant3.7$		
1310.9	$9/2^+$	783.5	$7/2^+$	$M1+E2$	$-0.16(8)$	0.14 ± 0.12	$3.6^{+1.4}_{-0.8}$	
		1310.9	$5/2^+$	$E2$		$1.8^{+0.7}_{-0.4}$		
1471.7	(7/2)	1471.7	$5/2^+$	$(M1+E2)$		$\leqslant6.5$[a]	$\leqslant1.0$[b]	
1487.8	$9/2^+$	960.4	$7/2^+$	$(M1+E2)$		$24.4^{+12.2a}_{-6.1}$	$30.0^{+15.0b}_{-7.5}$	
1536.6	$7/2^+$	447.1	$7/2^+$	$(M1+E2)$		103^{+65a}_{-44}	$27.4^{+13.6b}_{-10.9}$	
		1009.2	$7/2^+$	$M1+E2$	$-0.43(28)$	5.9 ± 5.6	36.9 ± 17.2	
		1536.6	$5/2^+$	$(M1+E2)$		0.59 ± 0.26[a]	1.8 ± 0.8[b]	
1623.3	(3/2)	903.5	$1/2^+$	$(M1+E2)$		$\leqslant205$[a]	$\leqslant223$[b]	
1710.7	$11/2^+$	1183.3	$7/2^+$	$E2$		5.6 ± 1.5		
1716.3	$(1/2,3/2)^+$	996.7	$1/2^+$	$(M1+E2)$		107 ± 21[a]	140 ± 29[b]	
		1716.3	$5/2^+$	$(M1+E2)$		28.7 ± 5.4[a]	113 ± 21[b]	
2040.1	$11/2^+$	552.3	$9/2^+$	$(M1+E2)$		118 ± 54[a]	48.2 ± 21.9[b]	
		1512.7	$7/2^+$	$E2$		0.60 ± 0.27		
2085.2		1557.9	$7/2^+$	$(M1+E2)$		28.3 ± 9.4[a]	91.6 ± 30.7[b]	
2187.6	$13/2^+$	426.3	$9/2^+$	$E2$		323^{+538}_{-142}		
		476.8	$11/2^+$	$(M1+E2)$		$\leqslant190$[a]	$\leqslant295$[b]	
		699.4	$9/2^+$	$E2$		$\leqslant27$		
		876.7	$9/2^+$	$E2$		$17.5^{+13.2}_{-6.9}$		
2228.7		917.8	$9/2^+$	$(M1+E2)$		$52.5^{+39.4a}_{-19.1}$	$58.9^{+44.2b}_{-21.5}$	
2300.0	$(1/2,3/2)^+$	1580.5	$1/2^+$	$(M1+E2)$		$2.0^{+2.5a}_{-0.9}$	$6.8^{+8.2b}_{-2.9}$	
		2300.0	$5/2^+$	$(M1+E2)$		$18.5^{+22.8a}_{-8.0}$	128^{+158b}_{-55}	
2323.3	$15/2^-$	1000.4	$11/2^-$	$E2$		$\leqslant8$		
2625.1	$17/2^+$	387.2	$15/2^+$	$M1+E2$	$+0.15(5)$	$36.3^{+29.4}_{-24.1}$	293^{+161}_{-87}	
		753.2	$13/2^+$	$E2$		$16.5^{+9.2}_{-5.0}$		
2778.8	$17/2^+$	591.2	$13/2^+$	$E2$		$\leqslant165$		
2841.7	17/2	316.8	$17/2^-$	$(M1+E2)$		644 ± 189[a]	8.7 ± 2.6[b]	
		519.0	$15/2^-$	$(M1+E2)$		92.2 ± 27.5[a]	33.1 ± 9.9[b]	
		604.4	$15/2^+$	$E1$				$(7.7\pm2.3)\times10^{-4}$
3214.7	$19/2^-$	141.5	$21/2^-$	$(M1+E2)$		$\leqslant17$[a]	$\leqslant44$[b]	
		372.4	$17/2^-$	$(M1+E2)$		$\leqslant570$[a]	$\leqslant120$[b]	
		589.6	$17/2^+$	$E1$				$\leqslant3.9\times10^{-4}$
		802.6	$15/2^-$	$E2$		$\leqslant0.5$		
		891.4	$15/2^-$	$E2$		$\leqslant5.2$		

[a]For pure $E2$ transition.
[b]For pure $M1$ transition.

deduced from the $B(E2;2_1^+\rightarrow0_1^+)$ values of the neighboring Sn cores [30], and a fermion effective charge of the same value was chosen. The fermion gyromagnetic ratios were $g_l=1.0$ and $g_s=3.91\ \mu_N$ (the proton free value quenched by a factor of 0.7), and for the boson gyromagnetic factor a value deduced from the average value of the magnetic moments of the 2_1^+ states in the Sn isotopes with mass from 116 to 124 ($\sim-0.22\mu_N$) [31]. The calculations of the one-proton transfer spectroscopic factors in the (^{3}He,d) reaction were based on the semimicroscopic transfer operator defined, e.g., in Ref. [32], and did not require additional parameters. The only adjustable parameter of the Hamiltonian of our calculations was Γ_0, the strength of the boson-fermion quadrupole-quadrupole interaction. The value used in the present calculations is $\Gamma_0=0.3$ MeV, slightly higher than the value 0.25 MeV of Refs. [20,21]. This value was optimized on the basis of the experimental excitation energies, transition probabilities, and proton transfer spectroscopic factors.

In the following, we present first a comparison of these calculations with the experimental data. Separate considerations will then be devoted to the ''intruder'' $9/2^+$ band, which cannot be described by the present IBFM calculations.

A. Comparison with the IBFM calculations

The positive parity calculated levels are shown in comparison with the experimental known levels in Fig. 4. As-

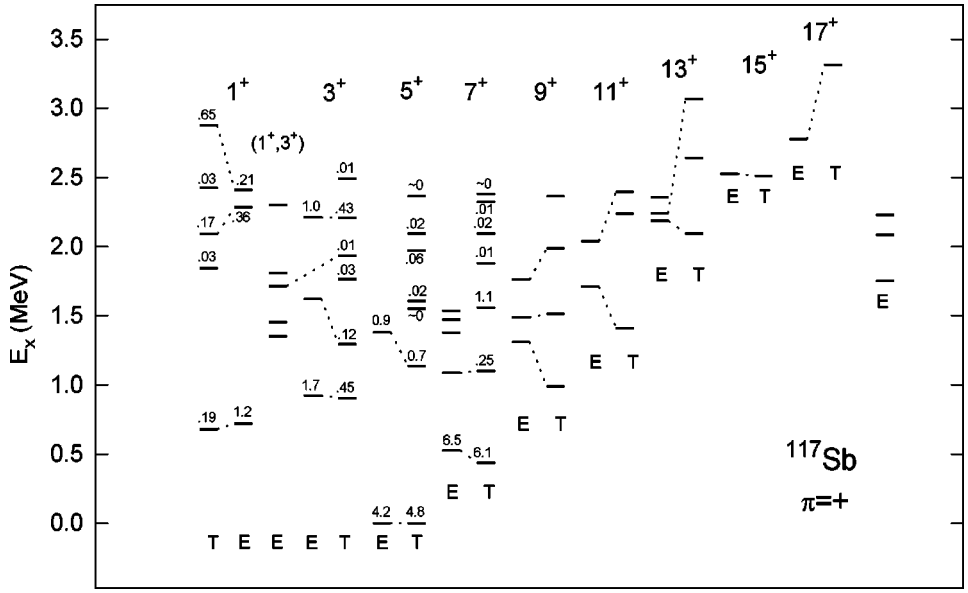

FIG. 4. Comparison between the experimental positive-parity levels in ^{117}Sb and the IBFM-1 present calculations (E and T denote the experimental and theoretical levels, respectively). The numbers labeling the levels with spins 1/2 up to 7/2 represent the spectroscopic factors of the (^{3}He,d) reaction [16-18]. Dashed lines indicate assignments of calculated levels to the experimental ones. To facilitate the understanding of the references from the text to this figure, we list below (in increasing order) the excitation energy (in keV) of all the experimental levels of each spin. $1/2^+$: 720, 2285, 2410; $1/2^+$,$3/2^+$: 1353, 1455, 1716, 1810, 2300; $3/2^+$: 924, 1623, 2213; $5/2^+$: 0.0, 1380; $7/2^+$: 527, 1089, (1379), 1472, 1537; $9/2^+$: 1311, 1487, 1761; $11/2^+$: 1711, 2040; $13/2^+$: 2188, 2242, 2356; $15/2^+$: 1527; $17/2^+$: 2778; unknown spin (to the right side): 1751, 2085, 2238. The intruder band based on the $9/2^+$ state at 1160 keV is not shown in this figure.

signed correspondences between experimental and calculated levels are indicated. These assignments are based on excitation energies, decay modes, and, when available, on the proton transfer spectroscopic factors in the (^{3}He,d) reaction. Table III completes Fig. 4 by providing detailed information on the electromagnetic decays.

The $1/2^+$ levels. The energy distribution of the $1/2^+$ states, as well as the fragmentation of the $s_{1/2}$ orbital stripping strength is generally well described. There are two states at 2285 and 2410 keV strongly populated in the (^{3}He,d) reaction, which can be easily assigned to two calculated states above 2 MeV which are also predicted with large spectroscopic factors. The first $1/2^+$ state, at 720 keV, is well described in energy, but its spectroscopic factor is underestimated. Its calculated structure is essentially $84\% d_{5/2}\otimes 2_1^+ + 12\% s_{1/2}\otimes 0_1^+$. In the lowest order of the proton transfer operator employed (when this is just the fermion creation operator) the too low spectroscopic factor would signify a too small $s_{1/2}\otimes 0_1^+$ component in the wave function of this state. However, it is not easy to bring a much larger component in the lowest $1/2^+$ state—its percentage increases slowly with increasing Γ_0, but at the same time the agreement for the rest of the states deteriorates rapidly. It is likely that the discrepancy noticed for this spectroscopic factor indicates the need of a more realistic transfer operator. Since the experimental lifetime of the $1/2_1^+$ state is not known, one cannot check, unfortunately, the $B(E2)$ value of its decay, which is predicted 13.0 W.u., comparable to that of the $2_1^+ \rightarrow 0_1^+$ transition of the core [17]. There are two other $1/2^+$ states predicted at about 1.8 and 2.5 MeV, with very small spectroscopic factors which are difficult to observe in the (^{3}He,d) reaction. The experimental 1810 keV, $(1/2,3/2)^+$ state may be tentatively assigned to the calculated $1/2_4^+$ state on the basis of its decay (Table III). There are also a few experimental states assigned as $1/2^+$, $3/2^+$, in the same range of excitation energies.

The $3/2^+$ levels. A few assignments could be made in this case. The first $3/2^+$ state is correctly predicted in position. Its spectroscopic factor is again underestimated by the theory, similarly to the case of the $1/2_1^+$ state. This state has a rather mixed structure: $16\% d_{3/2}\otimes 0_1^+ + (46\% d_{5/2} + 36\% g_{7/2})\otimes 2_1^+$. Its branching ratios are correctly predicted (Table III); unfortunately, the absence of the mixing ratio for its 924 keV transition to the ground state prevents a direct comparison with the calculated $B(E2)$ and $B(M1)$ values. We assign the state at 1623 keV as the calculated $3/2_2^+$ state, based on its strongest branch towards the $1/2_1^+$ state (Table III); however, as was predicted with a sizable spectroscopic factor but not observed in the (^{3}He,d) reaction, this assignment is only tentative. Other assignments are $3/2_4^+$ to the $1/2^+$, $3/2^+$ state at 1716 keV (on the basis of its γ decay), and $3/2_5^+$ to the 2213 keV state, on the basis of the strong spectroscopic factor. Although it is not possible to make a one to one correspondence for all $1/2^+$ and $3/2^+$ levels, one observes that the total number of levels with these spin values lying below about 2.5 MeV is well reproduced by the calculations.

The $5/2^+$ levels. The spectroscopic factor of the ground state is predicted very well; this is the ''parent'' $d_{5/2}$ state (calculated as 97% $d_{5/2}\otimes 0_1^+$). The state at 1380 keV, also strongly populated in the transfer reaction with $\ell=2$ (spin 3/2 or 5/2) is readily assigned to the $5/2_2^+$ calculated state. The γ decay of this state is not known. One should remark that there is another state at 1378.9 keV (assigned spin 7/2 [17]), observed in the $(p,n\gamma)$ reaction, which is believed to be different than the one at 1380 keV [17]. This level decays

TABLE III. Experimental and calculated (IBFM) branching ratios and transition probabilities in ^{117}Sb. Experimental decays and branching ratios are from Refs. [10,15,18]. The second column indicates the spin-parity and the order number of the calculated level assigned to the experimental one.

E_{lev} (keV)	J_i^π	J_f^π	E_γ (keV)	I_γ Calc.	I_γ Exp.	$B(E2)$ (W.u.) Calc.	$B(E2)$ (W.u.) Exp.	$B(M1)\times10^3$ (W.u.) Calc.	$B(M1)\times10^3$ (W.u.) Exp.
527.4	$7/2_1^+$	$5/2_1^+$	527.4	100	100	0.71		0.90	
719.5	$1/2_1^+$	$5/2_1^+$	719.5	100	100	13.0			
923.9	$3/2_1^+$	$5/2_1^+$	923.9	100	100	6.44	50 ± 15[a]	305	61 ± 20[b]
		$7/2_1^+$	396.5	0.03		6.18			
		$1/2_1^+$	204.4	0.8				239	
1089.4	$7/2_2^+$	$5/2_1^+$	1089.4	100	100	15.6	74 ± 38[a]	66.5	117 ± 60[b]
		$7/2_1^+$	562.0	0.02		0.19		0.08	
1310.9	$9/2_1^+$	$5/2_1^+$	1310.9	100	100	15.4	$1.8^{+0.7}_{-0.4}$		
		$7/2_2^+$	783.5	38.4	19.0	0.02	0.14 ± 0.12	63.7	$3.6^{+1.4}_{-0.8}$
		$7/2_2^+$	221.5	4.8		0.48		350	
1378.9	$5/2_2^+$	$5/2_1^+$	1378.9	100	[c]	13.4		35.6	
		$7/2_1^+$	851.5	7.9		0.17		23.2	
		$1/2_1^+$	659.4	0.1		1.02			
		$3/2_1^+$	455/0	14.2		0.02		274	
		$7/2_2^+$	289.5	8.4	[c]	1.71		631	
1487.3	$9/2_2^+$	$5/2_1^+$	1487.3	1.2		0.05			
		$7/2_1^+$	959.9	100	100	16.4	$24.4^{+12.2a}_{-6.1}$	26.7	$30.0^{+15.0b}_{-7.5}$
		$7/2_2^+$	397.9	0.1		0.18		0.94	
		$9/2_1^+$	176.4	2×10^{-4}		0.39		4×10^{-6}	
1536.6	$7/2_4^+$	$5/2_1^+$	1536.6	4.3	14.4	0.004	0.59 ± 0.26[a]	0.09	1.8 ± 0.8[b]
		$7/2_1^+$	1009.2	100	100	1.8	5.9 ± 5.6	5.81	37 ± 17
		$3/2_1^+$	612.7	16.4		12.0			
		$7/2_2^+$	447.2	41.5	5.6	1.04	103^{+65a}_{-44}	38.8	27^{+14b}_{-11}
		$9/2_1^+$	225.7	20.2		3.3		147	
		$9/2_2^+$	49.3	0.1		0.83		50.6	
1623.0	$3/2_2^+$	$5/2_1^+$	1623.0	93.2		8.4		30.8	
		$7/2_1^+$	1095.6	4.4		5.8			
		$1/2_1^+$	903.5	100	100	10^{-3}	$\leqslant205$[a]	375	$\leqslant223$[b]
		$3/2_1^+$	699.1	1.1		0.96		8.7	
		$5/2_2^+$	244.1	2.0		0.27		380	
1710.7	$11/2_1^+$	$7/2_1^+$	1183.3	100	100	15.7	5.6 ± 1.5		
		$9/2_2^+$	223.4	2.5		0.35		110	
1716.0	$3/2_4^+$	$5/2_1^+$	1716.0	100	100	0.01	27 ± 5[a]	31.4	108 ± 21[b]
		$7/2_1^+$	1188.6	1.8		0.90			
		$1/2_1^+$	996.5	28.9	24.9	0.48	101 ± 20[a]	45.8	6.9 ± 1.4[b]
		$3/2_1^+$	792.1	22.4		14.4		59.8	
		$5/2_2^+$	337.1	3.3		1.02		138	
1761.3	$9/2_3^+$	$5/2_1^+$	1761.3	0.7	26.1	7×10^{-4}			
		$7/2_1^+$	1233.9	2.8	29.0	0.06		0.21	
		$7/2_2^+$	671.9	100	100	7.9		68.7	
		$9/2_1^+$	450.4	1.9		14.4		0.70	
		$9/2_2^+$	274.0	2.2		0.01		23.9	
		$7/2_4^+$	224.7	2.5		4×10^{-4}		49.9	
1810.0	$1/2_4^+$	$5/2_1^+$	1810.0	64.7		0.07			
		$1/2_1^+$	1090.5	95.3	100	0		2.0	
		$3/2_1^+$	886.1	100	22.0	1.43		2.43	
		$5/2_2^+$	431.1	1.0		1.35			
		$3/2_2^+$	187.0	0.7		0.12		2.73	
		$3/2_4^+$	94.0	19.2		0.38		63.1	
2040.1	$11/2_3^+$	$7/2_1^+$	1512.7	4.1	23.0	0.02	0.60 ± 0.27		
		$7/2_2^+$	950.7	0.3		0.01			

TABLE III. (*Continued*).

E_{lev} (keV)	J_i^π	J_f^π	E_γ (keV)	I_γ Calc.	I_γ Exp.	$B(E2)$ (W.u.) Calc.	$B(E2)$ (W.u.) Exp.	$B(M1)\times10^3$ (W.u.) Calc.	$B(M1)\times10^3$ (W.u.) Exp.
		$9/2_1^+$	729.2	5.9		0.03		0.66	
		$9/2_2^+$	552.8	100	100	9.1	118 ± 54[a]	22.7	48 ± 22[b]
		$11/2_1^+$	329.4	2.1		13.2		0.77	
		$9/2_3^+$	278.8	0.1		0.07		0.011	
2187.6	$13/2_1^+$	$9/2_1^+$	876.7	100	100(25)	27.1	18^{+13}_{-7}		
		$9/2_2^+$	700.3	4×10^{-3}	$\leqslant50$	4×10^{-3}	$\leqslant27$		
		$11/2_1^+$	476.9	49.1	$\leqslant50$	0.03	$\leqslant190$[a]	84.9	$\leqslant295$[b]
		$9/2_3^+$	426.3	2×10^{-2}	50(25)	0.16	323^{+538}_{-142}		
		$11/2_3^+$	147.5	7×10^{-3}		7×10^{-6}		2.77	
2242.1	$13/2_3^+$	$11/2_1^+$	531.4	8.9		0.07		0.36	
		$9/2_3^+$	480.8	100	100	19.1			
		$11/2_3^+$	202.0	89.0		0.02		70.9	
2527.4	$15/2_1^+$	$11/2_1^+$	816.7	100	100	27.3			
2778.8	$17/2_1^+$	$13/2_1^+$	591.2	100	100	35.3	$\leqslant165$		
		$15/2_1^+$	251.4	42.2		0.03		89.9	

[a]For pure $E2$ transition.

[b]For pure $M1$ transition.

[c]Existing branch, but γ-ray intensity not known.

only to the $5/2^+$ g.s. and the 1089 keV $7/2^+$ level; this kind of decay is also reasonably well reproduced by the calculated $5/2_2^+$ level (Table III). This picture is consistent with the two levels 1378.9 and 1380 keV, being in fact the same level, assigned as $5/2_2^+$.

The 7/2$^+$ levels. The first $7/2^+$ state, at 527 keV is described also as the parent $g_{7/2}$ state ($93\%g_{7/2}\otimes0_1^+$), and its spectroscopic factor is well reproduced. The transition $7/2_1^+\rightarrow5/2_1^+$ is consequently predicted as a single-particle one (Table III). The second state, at 1089 keV, is assigned to the calculated $7/2_2^+$ state, its decay only to the g.s. being well reproduced. The calculations predict that the third 7/2 state has a large spectroscopic factor, but this state was not observed experimentally in the transfer reaction [17].

Higher spin positive-parity levels. All three known $9/2^+$ levels at 1311, 1487, and 1761 keV have been assigned to the first three calculated $9/2^+$ levels. Their decays are reasonably reproduced by the calculations. The yrast states above spin 9/2 are also reasonably well described (Fig. 4 and Table III). In addition, based on their decay, we assign the $11/2^+$ level at 2040 keV to $11/2_3^+$ and the $13/2^+$ level at 2242 keV to the $13/2_3^+$ calculated states, respectively.

A few considerations concerning the wave function structure of the lowest calculated states are given below. They are, generally, dominated by the $d_{5/2}$ and $g_{7/2}$ orbitals, the $s_{1/2}$ and $d_{3/2}$ ones being of relatively little importance.

As pointed out above, the $5/2_1^+$ and $7/2_1^+$ states, assigned to the g.s. and the 527.4 keV, respectively, are of a single-particle nature. The calculated states $1/2_1^+$, $3/2_1^+$, $5/2_2^+$, $7/2_2^+$, and $9/2_1^+$ have wave functions which indicate that they form, basically, the $d_{5/2}\otimes2_1^+$ multiplet; namely, their dominant configurations, in percentages of the $d_{5/2}$ and $g_{7/2}$ orbitals are (59,22), (46,36), (95,2), (93,6), and (95,1), respectively. The corresponding experimental multiplet is formed by the states at 719.5 keV ($1/2^+$), 923.9 keV ($3/2^+$), 1378.9 keV ($5/2^+$), 1089.4 keV ($7/2^+$), and 1310.9 keV ($9/2^+$). These states decay predominantly towards the g.s., by $B(E2)$ transition rates predicted, in general, of the order of the $B(E2;2_1^+\rightarrow0_1^+)$ value in the core (around 13 W.u.). As we can directly compare these values with the experimental ones, however, we remark that the experimental $B(E2;9/2_1^+\rightarrow5/2_1^+)$ value is definitely lower (less collective) than predicted. One can also observe (Fig. 4) that the position of this state is not described too well either. A possible reason for this fact, namely, the mixing of this state with the 1161 keV intruder $9/2^+$ state, will be discussed below.

The next expected multiplet $g_{7/2}\otimes2_1^+$ may be identified with the calculated $3/2_2^+$, $5/2_3^+$, $7/2_3^+$, $9/2_2^+$, and $11/2_1^+$ states, which have as dominant configurations (also in percentages of the $d_{5/2}$ and $g_{7/2}$ orbitals) (53,41), (51,43), (5,89), (8,91), and (4,91), respectively. As discussed above, only the experimental states 1487.3 keV ($9/2^+$) and 1710.7 keV ($11/2^+$), and possibly 1623.3 keV (3/2) have been assigned to this multiplet.

B. The intruder 9/2$^+$ band

As pointed out in the Introduction, the light odd Sb isotopes present systematically a low-lying band based on a $9/2^+$ state, which has a regular, rotational aspect (of a strongly coupled band). These bands have been interpreted as based on a $2p$-$1h$ proton configuration, namely, $(\pi g_{7/2}d_{5/2})^2\otimes(\pi g_{9/2})^{-1}$, which has a deformation β_2 of about 0.2 (see, for example, Ref. [10]). Our data on lifetimes of states from the intruder band allow a better characterization of this band.

TABLE IV. Experimental $B(\sigma L)$ values for the first two excited $9/2^+$ states in ^{115,117}Sb, compared to the values calculated with the cluster-vibration model (Ref. [33]). For clarity, the level with main configuration $d_{5/2}\otimes 2_1^+$ is labeled collective ($9/2_{\rm coll}$), whereas the bandhead of the intruder band is labeled intruder ($9/2_{\rm int}$). $9/2^+_{\rm coll}$: 1326 keV in ^{115}Sb and 1310 keV in ^{117}Sb. $9/2^+_{\rm int}$: 1381 keV in ^{115}Sb and 1160 keV in ^{117}Sb.

Transition		$B(E2)$ (W.u.)			$B(M1)\times 10^3$ (W.u.)		
J_i^π	J_f^π	^{117}Sb (exp.)	^{115}Sb (exp.)	^{115}Sb (calc.)	^{117}Sb (exp.)	^{115}Sb (exp.)	^{115}Sb (calc.)
$9/2^+_{\rm coll}$	$5/2^+_1$	2.0 ± 0.6	2.6 ± 0.4	5.0			
$9/2^+_{\rm coll}$	$7/2^+_1$	0.14 ± 0.12	0.50 ± 0.31	1.5×10^{-4}	3.9 ± 1.1	15 ± 3	39
$9/2^+_{\rm int}$	$5/2^+_1$	$\leqslant 3.7$	3.1 ± 1.3	1.3			
$9/2^+_{\rm int}$	$7/2^+_1$	$\leqslant 2.3$	0.23 ± 0.21	1.2×10^{-2}	$\leqslant 1.3$	20 ± 6	3.4

A first aspect concerns the lowest two $9/2^+$ states, one of them being the head of the intruder band. In this respect, the situation in ^{117}Sb is very similar to that discussed in detail for ^{115}Sb [21]. The $9/2^+$ state at 1310.9 keV is mainly the result of coupling a $d_{5/2}$ proton with the 2_1^+ state of ^{116}Sn, as discussed in the IBFM interpretation, while the first $9/2^+$ state, at 1160.3 keV, has been interpreted as the result of the promotion of a $g_{9/2}$ proton into a higher orbital, which gives a $2p$-$1h$ configuration of moderate deformation [10,33]. The two states are closely spaced and therefore may be mixed. Indication of this mixing are, as in the case of ^{115}Sb [21], the presence of the decay of both these states towards the $7/2_1^+$ state. For ^{115}Sb, the structure and decay of these two states was calculated within the cluster-vibrational model [34] which takes into account, in a unified manner, the coupling of both single-particle states and of a $2p$-$1h$ cluster with one-, two-, or three-phonon states of the Sn core. The predictions of this model for the absolute transition probabilities were found to be in reasonable agreement with experiment [21].

In the ^{117}Sb nucleus there are no such calculations, but, on the other hand, the experimental picture looks very similar to that of ^{115}Sb. Therefore, in Table IV we present the experimental situation of the decay of the first and second $9/2^+$ states in ^{117}Sb, compared to that from ^{115}Sb [21] and to the predictions of the cluster-vibration model [34]. One observes that the experimental B values, especially the $B(E2)$ ones, are very similar for these two nuclei. Since the model parameters for the existing calculations were taken from systematics and not from a particular fit, one may conclude that these calculations explain reasonably well, also in the case of ^{117}Sb, the mixing of the two $9/2^+$ states of very different basic configurations.

The second aspect concerns the deformation of the intruder band. This can be now determined from the $B(E2)$ value measured for the $17/2^+\rightarrow 13/2^+$ transition of this band (Table II) of $16.5^{+9.2}_{-5.0}$ W.u. ($0.056^{+0.031}_{-0.017}\ e^2\ {\rm b}^2$). By using the strong coupling formula [35]

$$B(E2;I+2\rightarrow I)=\frac{15}{32\pi}e^2Q_0^2\frac{(I+1-K)(I+1+K)(I+2-K)(I+2+K)}{(I+1)(2I+3)(I+2)(2I+5)}$$

we determine an intrinsic quadrupole moment of $Q_0=1.9\pm0.5$ b. Within the liquid drop model, with only axial quadrupole deformation, this corresponds to a deformation $\beta_2=0.14\pm0.07$. In a similar way, from the value $B(E2;19/2^+\rightarrow 15/2^+)=18.2\pm11.7$ W.u. in the intruder band of ^{115}Sb [21], one deduces an intrinsic quadrupole moment $Q_0=1.8\pm0.6$ b and a quadrupole deformation of $\beta_2=0.13\pm0.08$. These experimental values confirm the expected moderate deformation of $\varepsilon_2\approx0.15$ ($\beta_2\approx0.17$) for this band [33].

The structure of the intruder band in ^{115}Sb was also calculated in the framework of the hole-anharmonic core coupling model [36]. The lifetime predicted for the $17/2^+$ state of this band is $\tau=0.97-1.10$ ps. Although similar calculations for ^{117}Sb do not exist, we remark that this value agrees well with the experimental one measured in this work for the $17/2^+$ state, $1.4^{+0.6}_{-0.5}$ ps.

IV. SUMMARY

The use of the $(\alpha,2n\gamma)$ reaction allowed us to measure the lifetimes for a reasonable number of excited levels in ^{117}Sb, by using the Doppler shift attenuation method. The structure of this nucleus has been calculated with the interacting boson-fermion model. The assignments of calculated levels to the experimental ones were based on existing information, such as level energies, spin-parity values, electromagnetic decay modes (mainly branching ratios), and proton transfer spectroscopic factors. The positive parity states up to about 2.5 MeV excitation are reasonably well described by these IBFM calculations. The absolute transition rates determined in the present work could be compared to the calculated ones only in a few cases, due to the scarce experimental information on mixing ratios for the mixed $M1/E2$ transitions.

The present data support the picture of mixing between the lowest two excited $9/2^+$ states, one being a single particle ($d_{5/2}$) state, and the other an intruder $2p$-$1h$ state resulting from the excitation of a $g_{9/2}$ proton. The $B(E2)$ values determined from transitions in the $2p$-$1h$ intruder band in both ^{117}Sb (present work) and ^{115}Sb [21] are consistent with the expected moderate quadrupole deformation of this band.

ACKNOWLEDGMENT

This work was partly supported by a research grant from the Romanian Ministery for Science and Technology.

[1] R. E. Shroy, A. K. Gaigalas, G. Schatz, and D. B. Fossan, Phys. Rev. C **19**, 1324 (1979).
[2] V. P. Janzen, D. R. LaFosse, H. Schnare, D. B. Fossan, A. Galindo-Uribarri, J. R. Hughes, S. M. Mullins, E. S. Paul, L. Persson, S. Pilotte, D. C. Radford, I. Ragnarsson, P. Vaska, J. C. Waddington, R. Wadsworth, D. Ward, J. Wilson, and R. Wyss, Phys. Rev. Lett. **72**, 1160 (1994).
[3] T. Ishii, A. Makishima, M. Shibata, M. Ogawa, and M. Ishii, Phys. Rev. C **49**, 2982 (1994).
[4] H. Schnare, D. R. LaFosse, D. B. Fossan, J. R. Hughes, P. Vaska, K. Hauschild, I. M. Hibbert, R. Wadsworth, V. P. Janzen, D. C. Radford, S. M. Mullins, C. W. Beausang, E. S. Paul, J. DeGraaf, I. Y. Lee, A. O. Macchiavelli, A. V. Afanasjev, and I. Ragnarsson, Phys. Rev. C **54**, 1598 (1996).
[5] D. R. LaFosse, D. B. Fossan, J. R. Hughes, Y. Liang, H. Schnare, P. Vaska, M. P. Waring, J.y. Zhang, R. M. Clark, R. Wadsworth, S. A. Forbes, and E. S. Paul, Phys. Rev. C **50**, 1819 (1994).
[6] V. P. Janzen, H. R. Andrews, B. Haas, D. C. Radford, D. Ward, A. Omar, D. Prevost, M. Sawicki, P. Unrau, J. C. Waddington, T. E. Drake, A. Galindo-Uribarri, and R. Wyss, Phys. Rev. Lett. **70**, 1065 (1993).
[7] C.-B. Moon, S. J. Chae, J. H. Ha, T. Komatsubara, J. Lu, T. Hayakawa, and K. Furuno, Z. Phys. A **353**, 245 (1995).
[8] R. S. Chakrawarthy and R. G. Pillay, Phys. Rev. C **54**, 2319 (1996).
[9] D. R. LaFosse, D. B. Fossan, J. R. Hughes, Y. Liang, M. P. Waring, and J. y. Zhang, Phys. Rev. Lett. **69**, 1332 (1992).
[10] D. R. LaFosse, D. B. Fossan, J. R. Hughes, Y. Liang, H. Schnare, P. Vaska, M. P. Waring, and J. y. Zhang, Phys. Rev. C **56**, 760 (1997).
[11] W. D. Fromm, H. F. Brinckman, F. Donau, C. Heiser, F. R. May, V. V. Pashkevich, and H. Rotter, Nucl. Phys. **A243**, 9 (1975).
[12] K. Shafer, J. A. Carr, W. H. Kelly, W. C. McHarris, and R. A. Warner, Michigan State University Cyclotron Laboratory Annual Report, 1976, p. 85.
[13] T. J. Ketel, E. A. Z. M. Vervaet, and H. Verheul, Z. Phys. A **285**, 177 (1978).
[14] M. Ionescu-Bujor, A. Iordăchescu, G. Pascovici, and C. Stanescu, Nucl. Phys. **A466**, 317 (1987).
[15] Yu. N. Lobach and V. V. Trishin, Yad. Fiz. **58**, 1155 (1995).
[16] R. Kamermans, J. van Driel, H. P. Blok, and P. J. Blankert, Phys. Rev. C **17**, 1555 (1978).
[17] J. Blachot and G. Marguier, Nucl. Data Sheets **66**, 451 (1992).
[18] Evaluated Nuclear Structure Data File (ENSDF), maintained by the National Nuclear Data Center, Brookhaven National Laboratory.
[19] L. K. Kostov, W. Andrejtscheff, L. G. Kostova, A. Dewald, G. Bohm, K. O. Zell, P. von Brentano, H. Prade, J. Doring, and R. Schwengner, Z. Phys. A **337**, 407 (1990).
[20] D. Bucurescu, I. Căta-Danil, G. Ilaş, M. Ivaşcu, L. Stroe, and C. A. Ur, Phys. Rev. C **52**, 616 (1995).
[21] Yu. N. Lobach and D. Bucurescu, Phys. Rev. C **57**, 2880 (1998).
[22] I. Kh. Lemberg and A. A. Pasternak, *Modern Methods of Nuclear Spectroscopy* (Nauka, Leningrad, 1985).
[23] J. Lindhard, V. Nielsen, and M. Scharff, K. Dan. Vidensk. Selsk. Mat. Fys. Medd. **36**, 10 (1968).
[24] I. Kh. Lemberg and A. A. Pasternak, Nucl. Instrum. Methods **140**, 71 (1977).
[25] G. Van den Berghe and K. Heyde, Nucl. Phys. **A163**, 478 (1971).
[26] F. Iachello and O. Scholten, Phys. Rev. Lett. **43**, 679 (1979).
[27] B. S. Reehal and R. A. Sorensen, Phys. Rev. C **2**, 819 (1970).
[28] O. Scholten, computer codes ODDA and PBEM, KVI Internal Report No. 252, 1982.
[29] O. Scholten, computer code SPEC (unpublished).
[30] S. Raman, C. W. Nestor, S. Kahane, and K. H. Bhatt, At. Data Nucl. Data Tables **42**, 1 (1989).
[31] P. Raghavan, At. Data Nucl. Data Tables **42**, 189 (1989).
[32] O. Scholten and T. Ozzello, Nucl. Phys. **A424**, 221 (1984).
[33] K. Heyde, M. Waroquier, H. Vincx, and P. Van Isacker, Phys. Lett. **64B**, 135 (1976).
[34] J. Bron, W. H. A. Hesselink, H. Bedet, H. Verheul, and G. Van den Berghe, Nucl. Phys. **A279**, 365 (1977).
[35] H. Morinaga and T. Yamazaki, *In-beam Gamma-ray Spectroscopy* (North-Holland, Amsterdam, 1976), p. 198.
[36] P. Van Isacker, M. Waroquier, H. Vincx, and K. Heyde, Nucl. Phys. **A292**, 125 (1977).